

Violation of horizon by topological quantum excitations

I. Kukuljan,^{1,*} S. Sotiriadis,^{1,†} and G. Takács^{2,‡}

¹University of Ljubljana, Faculty of Mathematics and Physics, Jadranska ulica 19, SI-1000 Ljubljana, Slovenia

²BME “Momentum” Statistical Field Theory Research Group & BME

Department of Theoretical Physics, H-1117 Budapest, Budafoki út 8, Hungary

One of the fundamental principles of relativity is that a physical observable at any space-time point is determined only by events within its past light-cone. In non-equilibrium quantum field theory this is manifested in the way correlations spread through space-time: starting from an initially short-range correlated state, measurements of two observers at distant space-time points are expected to remain independent until their past light-cones overlap, resulting in the “horizon effect”. Surprisingly, we find that in the presence of topological excitations correlations can develop outside of horizon - even between infinitely distant points. We demonstrate this effect in the sine-Gordon model, showing that it can be attributed to the non-local nature of its topological excitations and interpret it as dynamical emergence of entanglement between distant regions of space.

Horizon effect in quantum field theory. Consider the following thought experiment: A system described by a quantum field theory (QFT) is prepared in some initial state and let to evolve under unitary relativistic dynamics. This can be realised by a paradigmatic protocol known as a “quantum quench” [1], in which a closed quantum system initially prepared in an equilibrium state undergoes a sudden change of its Hamiltonian at time $t = 0$. Let us suppose that the initial state is characterised by short-range correlations of local quantum fields with a small correlation length ξ ; such states are rather common and include ground and thermal states of massive QFTs. As a result, measurements made by two observers separated by a distance r will be independent until time $t \sim r/2c$, where c is the finite maximum speed at which information propagates [1, 2]. This is known as the “horizon effect” and can be justified by a semiclassical interpretation: correlations propagate by pairs of entangled quasiparticles emitted from initially correlated nearby points (at a distance $\lesssim \xi$) that travel to opposite directions with velocities limited by c . The horizon effect can be demonstrated in Conformal Field Theory for a class of initial states [1], and can be proved in the case of non-interacting relativistic dynamics for all initial states that satisfy the cluster decomposition property [3]. It also holds in lattice systems with local interactions due to the finite maximum velocity of quasi-particles [4] and it has been recently observed in cold atom experiments [5–7].

But what happens in the case of non-trivial interactions? It is known that interactions can have significant effects on the speed of propagation [8] or even fully suppress the spreading of correlations [9]. However, their interplay with the horizon effect remains incompletely understood. Here we address this question in the context of the sine-Gordon (SG) model

described by the Hamiltonian (using units in which $c = 1$)

$$H_{SG} = \int \left(\frac{1}{2} \Pi^2 + \frac{1}{2} (\partial_x \Phi)^2 - \frac{\mu^2}{\beta^2} \cos \beta \Phi \right) dx \quad (1)$$

where $[\Phi(x), \Pi(x')] = i\delta(x - x')$, μ is the mass parameter and β the interaction parameter of the theory. The SG model is a prototypical example of a 1+1 dimensional relativistic QFT with rich physics governed by topological excitations called solitons and antisolitons. They appear due to the periodic cosine potential compactifying the field to a circle topology $\Phi \sim \Phi + 2\pi/\beta$. Moreover, when the coupling parameter β is in the attractive regime $\beta^2 < 4\pi$, they form neutral bound states called breathers. The SG model has a non-trivial phase diagram with a transition of the Berezinskii-Kosterlitz-Thouless type at $\beta^2 = 8\pi$. It is an integrable model [10, 11] and describes the dynamics of numerous condensed matter systems [12]. The SG model has recently been realised in an ultra-cold atom experiment which enables the study of its correlation functions and non-equilibrium dynamics [13, 14]. Its dynamics has attracted considerable recent interest [15–20].

We prepare the system in an initial state $|\Omega\rangle$ with finite correlation length ξ and clustering property for local boson fields. The canonical case is the ground state of the massive Klein-Gordon (KG) Hamiltonian

$$H_{KG} = \int \left(\frac{1}{2} \Pi^2 + \frac{1}{2} (\partial_x \Phi)^2 + \frac{1}{2} m_0^2 \Phi^2 \right) dx \quad (2)$$

for which $\xi = 1/m_0$, while another case is the ground state of the SG model with parameters μ_0, β_0 . At time $t = 0$ we switch on SG dynamics with parameters μ, β and study the time evolution of connected correlations

$$C_{\mathcal{O}}(x, y; t) := \langle \Omega | e^{+iH_{SG}t} \mathcal{O}(x) \mathcal{O}(y) e^{-iH_{SG}t} | \Omega \rangle_{\text{conn}} \quad (3)$$

of local observables \mathcal{O} . We focus on three physically relevant observables: the field $\Phi(x)$ and its derivatives $\partial_x \Phi$ and $\partial_t \Phi = \Pi$ corresponding to the soliton density and current respectively. Although $\Phi(x)$ is an angular variable, its correlations are experimentally observable [13].

A surprise: out-of-horizon spreading of correlations. In order to study the dynamics of correlations we employ a recent variant [21] of a numerical method known as “Truncated Conformal Space Approach” (TCSA) [22] which is especially suited for the study of interacting 1+1 dimensional QFTs and efficiently captures non-perturbative effects (cf. Methods).

Fig. 1 shows the spreading of correlations under SG dynamics for increasing values of the interaction β . In marked contrast to the expected behaviour, SG dynamics leads to strong violations of the horizon effect: for small values of

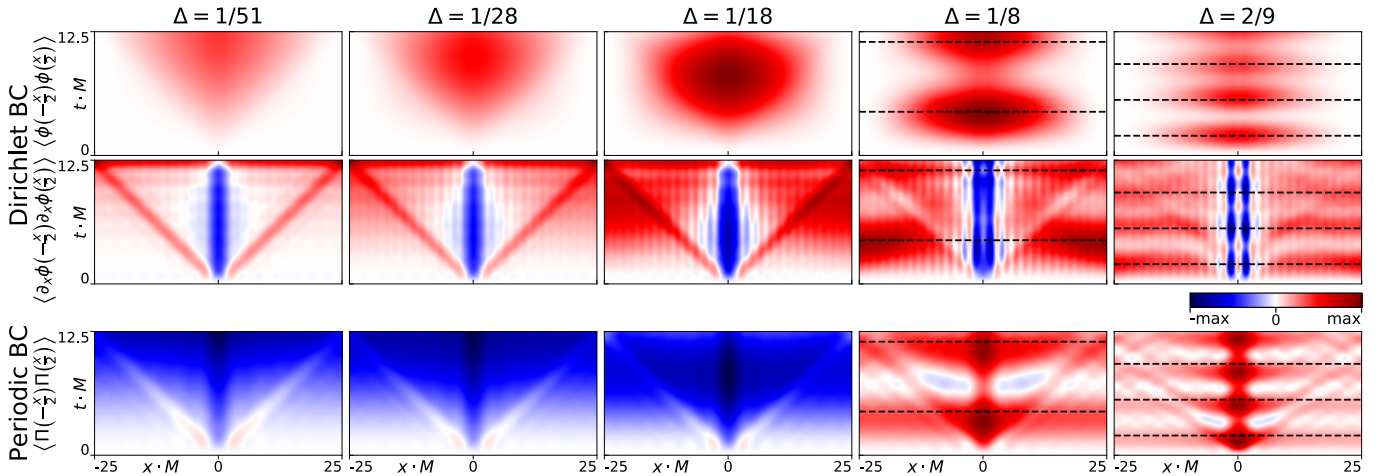


Figure 1. Density plots of connected correlations of Φ , $\partial_x \Phi$ and Π as functions of distance and time, obtained from TCSA simulation in a box with Dirichlet or periodic boundary conditions (DBC resp. PBC). The initial state is the KG ground state with mass m_0 in the DBC case or the SG ground state with first breather mass of equal magnitude $m_0 = 2M_0 \sin \pi \Delta / (2 - 2\Delta)$ for PBC. The dynamics corresponds to SG with soliton mass $M = 2.5 m_0$ and increasing values of the coupling parameter $\Delta = \beta^2 / 8\pi$. The horizontal dashed lines are plotted with a period corresponding to twice the first breather mass. Initial correlations have been subtracted from the result, and the box length is $L = 10 m_0^{-1}$.

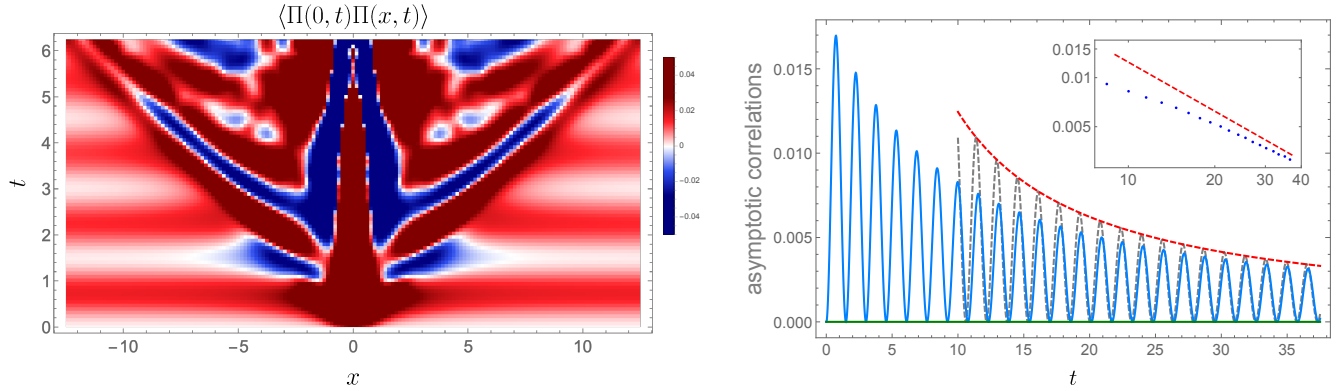


Figure 2. Analytical results for the correlations of Π under SG dynamics at $\beta = \sqrt{4\pi}$ for PBC. *Left*: Density plot of Π correlations as function of distance x and time t (in units $1/M$). Initial correlations have been subtracted as in Fig. 1. *Right*: Time evolution of the large distance asymptotics $\lim_{x \rightarrow \infty} \langle \Pi(0, t) \Pi(x, t) \rangle$ (blue line) together with their large time scaling $\sim \sin^2(2Mt)/t$ and envelope (gray and red dashed lines respectively). The vanishing large distance asymptotics of $\partial_x \Phi$ correlations (green line) are included for completeness. *Right inset*: log-log plot showing the large time scaling of asymptotic Π correlations. The points are the maxima of the oscillations and the red dashed line the $\sim 1/t$ envelope. The initial state is the KG ground state with mass m_0 and the post-quench soliton mass is $M = 2.5m_0$.

β the correlations stay within or close to the horizon, while for larger β they quickly spread outside of the horizon, and develop temporal oscillations at a frequency increasing with β . We find that the violation of horizon is present universally in quenches to the SG model, independently of the initial state studied [3]. It is most drastic for the derivative fields $\partial_x \Phi$ and $\partial_t \Phi = \Pi$, for which the out-of-horizon correlations become spatially uniform for large distance. The observed phenomenon has an interesting dependence on the boundary conditions: in case of Dirichlet boundary conditions (DBC) the violation is dominantly in the $C_{\partial_x \Phi}$ channel, while for periodic boundary conditions (PBC) the violation is dominated by the C_{Π} correlations, which are shown in Fig. 1 (the other correlations can be found in the SI [3]).

Explanation. To validate our unexpected numerical observation and clarify the origins of the out-of-horizon effect,

we perform an analytical calculation of the dynamics at a convenient value of the coupling, exploiting the powerful tool of bosonisation [23, 24] (cf. Methods).

Bosonisation provides an exact non-linear and non-local correspondence between a fermionic and a bosonic QFT in 1+1 dimensions. It relates the SG model to an interacting fermionic QFT, the massive Thirring model [25], where the soliton-antisoliton fields of SG are identified with the fermion fields [26] (cf. Eq. (6) in Methods). In particular, for the strongly interacting case $\beta^2 = 4\pi$ of the SG model, the fermion interaction vanishes and the SG model becomes equivalent to the free massive Dirac theory

$$H_{MF} = \int \bar{\Psi} (-i\gamma^1 \partial_x + M) \Psi dx, \quad (4)$$

which enables analytic calculation of the time evolution.

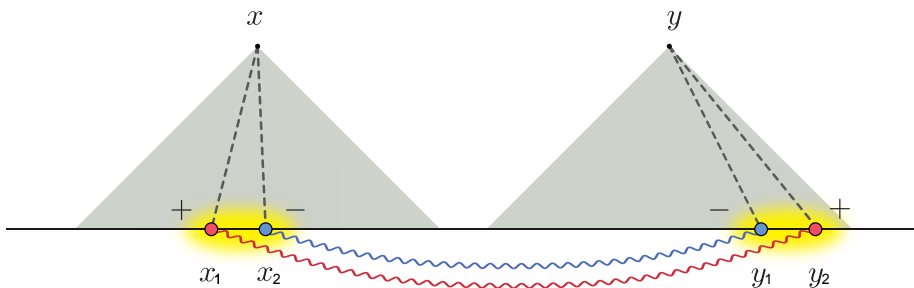


Figure 3. Graphical explanation of how a non-zero out-of-horizon correlation $C_{\Pi}(x, y; t)$ emerges due to the presence of long-range initial fermionic correlations. The coloured links depict the correlation $C_{+-+}^F(x_1, x_2, y_1, y_2)$, while the black dashed lines are the fermion (i.e. soliton) propagators. The yellow regions show the correlation length m_0^{-1} of the pre-quench KG model.

Using bosonisation, we compute the dynamics of correlations in the KG-to-SG quench for periodic BC in the thermodynamic limit, in the following steps: (1) fermionising the SG model and expressing the observables \mathcal{O} in terms of the fermion field Ψ of the Thirring model (cf. Eq. (9) and (10) in Methods); (2) time evolving the fermion field and expressing the dynamical fermion correlations in terms of initial ones; and (3) deriving the fermionic initial correlations in the KG ground state $|\Omega\rangle$ from the bosonic ones.

The resulting exact time evolution of C_{Π} is shown in Fig. 2. The analytical results confirm the dynamical emergence of out-of-horizon connected correlations, which are only present for the field $\Pi(x)$ and not for $\partial_x\Phi(x)$, consistently with the numerical TCSA results. Note that the horizon violation persists up to infinite distances and its long range asymptotics exhibits oscillations algebraically decaying with time.

Bosonisation provides a transparent explanation for the observed effect. The correlation functions $C_{\partial_x\Phi}(x, y; t)$ and $C_{\Pi}(x, y; t)$ can be expressed as quadruple convolutions of the free fermion propagator $G_{\sigma\rho}(x - x', t)$ (cf. eqs. (12) and (13) in Methods) with the initial four-point correlations of the fermion fields on the KG ground state $|\Omega\rangle$. The indices σ, ρ, \dots correspond to the two fermion field components labelled by \pm . The fermion propagators vanish identically outside of the light-cone ($|x - x'| > t$) so they cannot be the source of the horizon violation.

The initial fermionic correlations, however, display unexpected behaviour which is where the observed effect originates from. Among the six terms allowed by the fermionic superselection rules, two of them,

$$C_{\pm\mp\mp\pm}^F := \langle \Omega | \Psi_{\pm}^{\dagger}(x) \Psi_{\mp}(x+a) \Psi_{\mp}^{\dagger}(y) \Psi_{\pm}(y+b) | \Omega \rangle \quad (5)$$

violate the cluster decomposition principle. That is, these terms do not factorise to a product of two-point functions asymptotically as $|x - y| \rightarrow \infty$. More precisely, $C_{\pm\mp\mp\pm}^F$ tends to a nonzero value in this limit while the two-point functions vanish. Due to the non-locality of the fermionic fields such correlations are undetectable by local measurements in the initial state, which has short-range correlations for the observable bosonic local fields. However, the long-range correlations of the fermionic (i.e. solitonic) degrees of freedom are made manifest in the correlations of local fields for $t > 0$, due

to the interacting dynamics of the SG model, and dominate the asymptotic correlations of Π .

Discussion. We stress that the horizon violation effect is entirely compatible with all relevant physical principles: there is no contradiction with relativistic causality since the retarded propagator vanishes outside the causal cone. In the initial equilibrium state the cluster decomposition property is only violated for a non-local (fermionic) field. For $t > 0$ it is also violated for local fields such as $\partial_x\Phi$ and $\partial_t\Phi$, but the system is no longer at equilibrium.

Relativistically invariant dynamics and exponential clustering of initial correlations are sufficient conditions to prove the presence of horizon when dynamics is free in terms of the local fields [3]. However, the SG dynamics is governed by topologically non-trivial solitonic excitations, which are created by fields non-local in terms of the bosonic fields. Therefore short range bosonic correlations in the initial state do not preclude long-distance entanglement of such quasi-particle pairs created during the quantum quench. The observed boundary dependence is another signature of the topological origin of the effect, as the dynamics of topological excitations is always strongly dependent on the boundary conditions.

It might appear counter-intuitive that two observers located far away from each other experience correlated measurements immediately after $t = 0$. This can be understood as a quantum field theoretic manifestation of long-distance entanglement of the Einstein-Podolsky-Rosen (EPR) type [27]: the asymptotic nonvanishing of $C_{\pm\mp\mp\pm}^F$ can be interpreted as long-distance entanglement between soliton – anti-soliton pairs, as depicted in Fig. 3. Just as in the case of EPR, local commutativity of observables still holds, therefore these infinite distance correlations are compatible with relativity.

The out-of-horizon spreading of correlations uncovered here provides a mechanism to produce infinite-range correlations in QFT. In addition, it is a concrete prediction for experiments realising SG dynamics such as in [13]. It is also expected to be a general feature of non-equilibrium dynamics in topological phases of quantum condensed matter systems and other QFTs with non-trivial target space topology.

Acknowledgments. This work was partially supported by the Advanced Grant of European Research Council (ERC) 694544 – OMNES, by the Slovenian Research Agency under

grants N1-0055 (OTKA-ARRS joint grant) and P1-0402, as well as by the National Research Development and Innovation Office of Hungary within the Quantum Technology National Excellence Program (Project No. 2017-1.2.1-NKP-2017-00001) and under grants OTKA No. SNN118028 and K-16 No. 119204. S.S. acknowledges support by the Slovenian Research Agency under grant N1-0109 (QTE). The work of G.T. was also partially supported by the BME-Nanotechnology FIKP grant of EMMI (BME FIKP-NAT). I.K. is grateful to Martin Horvat for support in high-performance computing.

* ivan.kukuljan@mf.uni-lj.si

† spyridon.sotiriadis@mf.uni-lj.si

‡ takacs@eik.bme.hu

- [1] P. Calabrese and J. Cardy, “Time Dependence of Correlation Functions Following a Quantum Quench,” *Physical Review Letters* **96** no. 13, (2006) 136801.
- [2] F. Iglói and H. Rieger, “Long-Range Correlations in the Nonequilibrium Quantum Relaxation of a Spin Chain,” *Phys. Rev. Lett.* **85** no. 15, (2000) 3233–3236.
- [3] See Supplementary Information for details.
- [4] E. H. Lieb and D. W. Robinson, “The finite group velocity of quantum spin systems,” *Comm. Math. Phys.* **28** no. 3, (1972) 251–257.
- [5] M. Cheneau, P. Barmettler, D. Poletti, M. Endres, P. Schauf, T. Fukuhara, C. Gross, I. Bloch, C. Kollath, and S. Kuhr, “Light-cone-like spreading of correlations in a quantum many-body system,” *Nature (London)* **481** no. 7382, (2012) 484–487.
- [6] T. Langen, R. Geiger, M. Kuhnert, B. Rauer, and J. Schmiedmayer, “Local emergence of thermal correlations in an isolated quantum many-body system,” *Nature Physics* **9** (2013) 640–643.
- [7] P. Jurcevic, B. P. Lanyon, P. Hauke, C. Hempel, P. Zoller, R. Blatt, and C. F. Roos, “Quasiparticle engineering and entanglement propagation in a quantum many-body system,” *Nature (London)* **511** no. 7508, (2014) 202–205.
- [8] L. Bonnes, F. H. L. Essler, and A. M. Läuchli, ““Light-Cone” Dynamics After Quantum Quenches in Spin Chains,” *Phys. Rev. Lett.* **113** no. 18, (2014) 187203.
- [9] M. Kormos, M. Collura, G. Takács, and P. Calabrese, “Real-time confinement following a quantum quench to a non-integrable model,” *Nature Physics* **13** (2017) 246–249.
- [10] A. B. Zamolodchikov, “Exact two-particle S-matrix of quantum sine-Gordon solitons,” *Communications in Mathematical Physics* **55** no. 2, (1977) 183–186.
- [11] A. B. Zamolodchikov and A. B. Zamolodchikov, “Factorized S-matrices in two dimensions as the exact solutions of certain relativistic quantum field theory models,” *Annals of Physics* **120** no. 2, (1979) 253–291.
- [12] T. Giamarchi, *Quantum Physics in One Dimension*. Clarendon Press, 2003.
- [13] T. Schweigler, V. Kasper, S. Erne, I. Mazets, B. Rauer, F. Cataldini, T. Langen, T. Gasenzer, J. Berges, and J. Schmiedmayer, “Experimental characterization of a quantum many-body system via higher-order correlations,” *Nature* **545** no. 7654, (2017) 323–326.
- [14] M. Pigneur, T. Berrada, M. Bonneau, T. Schumm, E. Demler, and J. Schmiedmayer, “Relaxation to a Phase-Locked Equilibrium State in a One-Dimensional Bosonic Josephson Junction,” *Physical Review Letters* **120** no. 17, (2018) 173601.
- [15] K. Damle and S. Sachdev, “Universal Relaxational Dynamics of Gapped One-Dimensional Models in the Quantum Sine-Gordon Universality Class,” *Physical Review Letters* **95** no. 18, (2005) 187201.
- [16] E. G. Dalla Torre, E. Demler, and A. Polkovnikov, “Universal Rephasing Dynamics after a Quantum Quench via Sudden Coupling of Two Initially Independent Condensates,” *Physical Review Letters* **110** no. 9, (2013) 090404.
- [17] B. Bertini, D. Schuricht, and F. H. L. Essler, “Quantum quench in the sine-Gordon model,” *Journal of Statistical Mechanics: Theory and Experiment* **10** (2014) 10035.
- [18] M. Kormos and G. Zaránd, “Quantum quenches in the sine-Gordon model: A semiclassical approach,” *Phys. Rev. E* **93** no. 6, (2016) 062101.
- [19] C. P. Moca, M. Kormos, and G. Zaránd, “Hybrid Semiclassical Theory of Quantum Quenches in One-Dimensional Systems,” *Physical Review Letters* **119** no. 10, (2017) 100603.
- [20] D. X. Horváth, I. Lovas, M. Kormos, G. Takács, and G. Zaránd, “Nonequilibrium time evolution and rephasing in the quantum sine-Gordon model,” *Physical Review A* **100** no. 1, (2019) 013613.
- [21] I. Kukuljan, S. Sotiriadis, and G. Takács, “Correlation Functions of the Quantum Sine-Gordon Model in and out of Equilibrium,” *Physical Review Letters* **121** no. 11, (2018) 110402.
- [22] V. P. Yurov and A. B. Zamolodchikov, “Truncated Conformal Space Approach to scaling Lee-Yang model,” *International Journal of Modern Physics A* **05** no. 16, (1990) 3221–3245.
- [23] J. von Delft and H. Schoeller, “Bosonization for beginners - refermionization for experts,” *Annalen der Physik* **7** no. 4, (1998) 225–305.
- [24] A. Gogolin, A. Nersisyan, and A. Tsvelik, *Bosonization and Strongly Correlated Systems*. Cambridge University Press, 2004.
- [25] S. Coleman, “Quantum sine-Gordon equation as the massive Thirring model,” *Physical Review D* **11** no. 8, (1975) 2088–2097.
- [26] S. Mandelstam, “Soliton operators for the quantized sine-Gordon equation,” *Physical Review D* **11** no. 10, (1975) 3026–3030.
- [27] A. Einstein, B. Podolsky, and N. Rosen, “Can quantum-mechanical description of physical reality be considered complete?,” *Phys. Rev.* **47** (1935) 777–780.
- [28] A. J. A. James, R. M. Konik, P. Lecheminant, N. J. Robinson, and A. M. Tsvelik, “Non-perturbative methodologies for low-dimensional strongly-correlated systems: From non-Abelian bosonization to truncated spectrum methods,” *Reports on Progress in Physics* **81** no. 4, (2018) 046002.
- [29] T. Rakovszky, M. Mestyán, M. Collura, M. Kormos, and G. Takács, “Hamiltonian truncation approach to quenches in the Ising field theory,” *Nuclear Physics B* **911** (2016) 805–845.
- [30] G. Feverati, F. Ravanini, and G. Takács, “Truncated conformal space at $c = 1$, nonlinear integral equation and quantization rules for multi-soliton states,” *Physics Letters B* **430** no. 3–4, (1998) 264–273.
- [31] P. Calabrese and J. Cardy, “Quantum quenches in extended systems,” *Journal of Statistical Mechanics: Theory and Experiment* **2007** no. 06, (2007) P06008.
- [32] A. M. Läuchli and C. Kollath, “Spreading of correlations and entanglement after a quench in the one-dimensional Bose Hubbard model,” *Journal of Statistical Mechanics: Theory and Experiment* **2008** no. 5, (2008) 05018.

- [33] S. R. Manmana, S. Wessel, R. M. Noack, and A. Muramatsu, “Time evolution of correlations in strongly interacting fermions after a quantum quench,” *Phys. Rev. B* **79** no. 15, (2009) 155104.
- [34] G. Carleo, F. Becca, L. Sanchez-Palencia, S. Sorella, and M. Fabrizio, “Light-cone effect and supersonic correlations in one- and two-dimensional bosonic superfluids,” *Phys. Rev. A* **89** no. 3, (2014) 031602.
- [35] L. Bonnes, F. H. L. Essler, and A. M. Läuchli, ““Light-Cone” Dynamics After Quantum Quenches in Spin Chains,” *Phys. Rev. Lett.* **113** no. 18, (2014) 187203.
- [36] A. B. Zamolodchikov, “Mass scale in the sine-Gordon model and its reductions,” *International Journal of Modern Physics A* **10** no. 08, (1995) 1125–1150.
- [37] A. Iucci and M. A. Cazalilla, “Quantum quench dynamics of the sine-Gordon model in some solvable limits,” *New Journal of Physics* **12** no. 5, (May, 2010) 055019.
- [38] B. Bertini, D. Schuricht, and F. H. L. Essler, “Quantum quench in the sine-Gordon model,” *Journal of Statistical Mechanics: Theory and Experiment* **2014** no. 10, (2014) P10035.
- [39] A. C. Cubero and D. Schuricht, “Quantum quench in the attractive regime of the sine-Gordon model,” *Journal of Statistical Mechanics: Theory and Experiment* **2017** no. 10, (2017) 103106.
- [40] D. Horváth and G. Takács, “Overlaps after quantum quenches in the sine-Gordon model,” *Physics Letters B* **771** (2017) 539–545.
- [41] C. Rylands and N. Andrei, “Loschmidt amplitude and work distribution in quenches of the sine-Gordon model,” *Physical Review B* **99** no. 8, (Feb., 2019) 085133.
- [42] J. Mossel and J.-S. Caux, “Exact time evolution of space- and time-dependent correlation functions after an interaction quench in the one-dimensional Bose gas,” *New Journal of Physics* **14** no. 7, (July, 2012) 075006.
- [43] M. Kormos, M. Collura, and P. Calabrese, “Analytic results for a quantum quench from free to hard-core one-dimensional bosons,” *Physical Review A* **89** no. 1, (Jan., 2014) 013609.
- [44] S. Sotiriadis and P. Calabrese, “Validity of the GGE for quantum quenches from interacting to noninteracting models,” *Journal of Statistical Mechanics: Theory and Experiment* **2014** no. 7, (July, 2014) P07024.
- [45] S. Sotiriadis, “Equilibration in one-dimensional quantum hydrodynamic systems,” *Journal of Physics A: Mathematical and Theoretical* **50** no. 42, (Sept., 2017) 424004.
- [46] A. Bastianello, M. Collura, and S. Sotiriadis, “Quenches from bosonic Gaussian initial states to the Tonks-Girardeau limit: Stationary states and effects of a confining potential,” *Physical Review B* **95** no. 17, (May, 2017) 174303.
- [47] I. Gradshteyn and I. Ryzhik, *Table of Integrals, Series, and Products*. Academic Press, 2007.

Methods. The dynamics of correlations was computed using two complementary methods, the numerical “Truncated Conformal Space Approach” (TCSA) and the analytical approach of bosonisation.

Truncated Conformal Space Approach. The TCSA [22] is a numerical method for the non-perturbative study of (1+1)-dimensional QFT models (cf. [28] for a recent review) and recently extended to non-equilibrium time evolution [21, 29]. It assumes that the Hamiltonian can be written as $H = H_0 + \Delta H$ where H_0 is exactly solvable, while ΔH is an operator with known matrix elements between eigenstates of H_0 . Truncating the Hilbert space by an energy cut-off in finite volume L , it becomes finite dimensional.

For the SG model (1) the reference Hamiltonian H_0 is the massless free boson Conformal Field Theory (CFT) $H_{CFT} = \int (\frac{1}{2}\Pi^2 + \frac{1}{2}(\partial_x\Phi)^2)dx$ and the perturbing operator is $\Delta H = -\frac{\mu}{\beta^2} \int \cos\beta\Phi dx$ [30]. For $\beta^2 < 8\pi$ the operator $\cos\beta\Phi$ is a relevant scaling operator and so the effective coupling flows to zero at high energy, therefore the numerical results are expected to converge with the cut-off, with a rate dependent on β ; for sufficiently attractive couplings the method converges very fast. The evolution is followed for times up to $t = L/2$ to avoid boundary effects arising from the finite volume.

The numerical simulation consists of the following steps:

1. Constructing truncated matrix representations of the pre-quench and post-quench Hamiltonians;
2. Computing the initial state $|\Omega\rangle$ in the CFT basis, as the ground state of the pre-quench Hamiltonian;
3. Computing the time evolution operator $\exp(-iH_{SG}t)$ by matrix exponentiation;
4. Constructing the observables Φ , $\partial_x\Phi$ and Π at different positions in space using mode expansions in the CFT basis;
5. Evaluating the correlation functions as expectation values $\langle\Omega|e^{+iH_{SG}t}\mathcal{O}(x)\mathcal{O}(y)e^{-iH_{SG}t}|\Omega\rangle$, and determining the connected correlations $C_{\mathcal{O}}(x, y; t)$.

We stress that the KG Hamiltonian, as well as correlations involving Φ are not generally possible to implement in TCSA due to infrared divergences from the massless boson zero mode; Dirichlet boundary conditions are an exception because the zero mode is absent.

Bosonisation/fermionisation. As discovered in [25], the massive Thirring model described by the Hamiltonian

$$H_{MT} = \int [\bar{\Psi}(-i\gamma^1\partial_x + M)\Psi + \frac{1}{2}g(\bar{\Psi}\gamma^\mu\Psi)(\bar{\Psi}\gamma_\mu\Psi)] dx$$

is equivalent to the SG model (1) with

$$\frac{\beta^2}{4\pi} = \frac{1}{1 + g/\pi},$$

where the fermion mass M is identified with the SG soliton mass. The interacting fermion fields Ψ_{\pm} create the soliton/anti-soliton excitations and can be written as a non-local expression of the SG fields $\Phi(x)$ and $\Pi(x)$ [26]:

$$\Psi_{\pm}(x) = \mathcal{N} : \exp\left[-\frac{2\pi i}{\beta} \int_{-\infty}^x d\xi \Pi(\xi) \mp \frac{i\beta}{2}\Phi(x)\right] : \quad (6)$$

where \mathcal{N} is a normalisation constant, and $:$ denotes normal ordering. For $\beta^2 = 4\pi$ the fermion interaction g vanishes and (6) simplifies to

$$\Psi_{\pm}(x) = \mathcal{N} :e^{\mp\sqrt{4\pi i}\mathcal{X}_{\pm}(x)}: \quad (7)$$

where

$$\mathcal{X}_{\pm}(x) = \frac{1}{2} \left(\Phi(x) \pm \int_{-\infty}^x dx' \Pi(x') \right), \quad (8)$$

with the inverse relation given by

$$\partial_x \mathcal{X}_{\pm}(x) = \mathcal{N}' : \Psi_{\pm}^{\dagger}(x) \Psi_{\pm}(x) : \quad (9)$$

Our analytical calculation consists of:

1. Fermionising the SG model and rewriting the observables in terms of the fermionic fields using the inverse of (8)

$$\partial_x \Phi = \partial_x \mathcal{X}_+ + \partial_x \mathcal{X}_-, \quad \Pi = \partial_x \mathcal{X}_+ - \partial_x \mathcal{X}_-, \quad (10)$$

together with (9);

2. Deriving the time evolved correlations $C_{\partial\Phi}(x, y; t)$ and $C_{\Pi}(x, y; t)$ from the initial fermionic correlations by:

(a) solving the free fermion time evolution

$$\dot{\Psi}_{\sigma} = \sigma \partial_x \Psi_{\sigma} + iM \Psi_{-\sigma}$$

in terms of initial conditions for the field as

$$\Psi_{\sigma}(x, t) = \sum_{\sigma'=\pm} \int dx' G_{\sigma\sigma'}(x-x', t) \Psi_{\sigma'}(x', 0) \quad (11)$$

where $G_{\sigma\sigma'}(x-x', t)$ is the retarded Green's function;

(b) using (11) to express the time evolution of bosonic correlations in terms of the initial fermionic correlations:

$$\begin{aligned} \left\{ \begin{array}{l} C_{\partial_x \Phi}(x, y; t) \\ C_{\Pi}(x, y; t) \end{array} \right\} &= \mathcal{N}'^2 \sum_{\sigma_i, \rho_i=\pm} \left\{ \begin{array}{l} 1 \\ \sigma_0 \rho_0 \end{array} \right\} \int dx_1 dx_2 dy_1 dy_2 \\ &\times G_{\sigma_0 \sigma_1}^*(x-x_1, t) G_{\sigma_0 \sigma_2}(x-x_2, t) G_{\rho_0 \rho_1}^*(y-y_1, t) \\ &\times G_{\rho_0 \rho_2}(y-y_2, t) \left(C_{\sigma_1 \sigma_2 \rho_1 \rho_2}^F(x_1, x_2, y_1, y_2) \right. \\ &\left. - C_{\sigma_1 \sigma_2}^F(x_1, x_2) C_{\rho_1 \rho_2}^F(y_1, y_2) \right), \quad (12) \end{aligned}$$

3. Deriving the initial fermionic correlations

$$\begin{aligned} C_{\sigma\sigma'\rho\rho'}^F(x, x', y, y') &:= \langle \Omega | \Psi_{\sigma}^{\dagger}(x) \Psi_{\sigma'}(x') \Psi_{\rho}^{\dagger}(y) \Psi_{\rho'}(y') | \Omega \rangle \\ C_{\sigma\sigma'}^F(x, x') &:= \langle \Omega | \Psi_{\sigma}^{\dagger}(x) \Psi_{\sigma'}(x') | \Omega \rangle \quad (13) \end{aligned}$$

in the KG ground state $|\Omega\rangle$ as follows:

- (a) identifying the index combinations $\sigma, \sigma', \rho, \rho'$ allowed by fermionic superselection rules;
- (b) expressing fermionic correlations $C_{\sigma\sigma'\rho\rho'}^F(x, x', y, y')$ in terms of bosonic ones $\langle \Omega | \mathcal{X}_{\sigma}(x) \mathcal{X}_{\sigma'}(x') | \Omega \rangle$ using (7) and exploiting the Gaussianity of $|\Omega\rangle$ in terms of the bosonic fields via Wick's theorem;
- (c) obtaining correlators $\langle \Omega | \mathcal{X}_{\sigma}(x) \mathcal{X}_{\sigma'}(x') | \Omega \rangle$ from those of Φ and Π using (8).

Finally we integrate numerically (12) to get $C_{\partial_x \Phi}(x, y; t)$ and $C_{\Pi}(x, y; t)$ for finite $r = |x-y|$, and compute analytically the asymptotics at large r for any time t to verify the horizon violation effect explicitly.

The interested reader can find further details in the SI.

SUPPLEMENTARY INFORMATION

This Supplementary Information includes the following sections:

- **Proof of horizon effect for free dynamics and local initial states** – showing in a transparent way how the horizon effect is proven in case of free QFT and how it depends on the necessary conditions stated in the main text.
- **Further numerical results** – listing further numerical evidence for the properties of the horizon violation claimed in the main text.
- **Analytical demonstration of the out-of-horizon effect** – a detailed exposition of the analytical proof of the horizon violation in Klein-Gordon to sine-Gordon quenches at $\beta = \sqrt{4\pi}$.

Proof of horizon effect for free dynamics and local initial states

The horizon or lightcone effect after a quantum quench was pointed out in [1, 2, 31] and explained through a quasiparticle interpretation. In this description the quench initial state acts as a source of entangled pairs of quasiparticles that originate from points at a distance smaller or of the order of the initial correlation length and travel ballistically to opposite directions, spreading correlations through the system. Therefore correlations between two points start developing only when the fastest pair of quasiparticles that originate from the middle reach both points, which happens at time $t \sim r/2c$. Several subsequent works verified the presence of horizon both analytically and numerically [8, 32–35], especially in lattice systems with local couplings and interactions, whose dynamics, even though not relativistically invariant, is still constrained by a maximum velocity of information propagation [4], and it has also been observed in experiments [5–7].

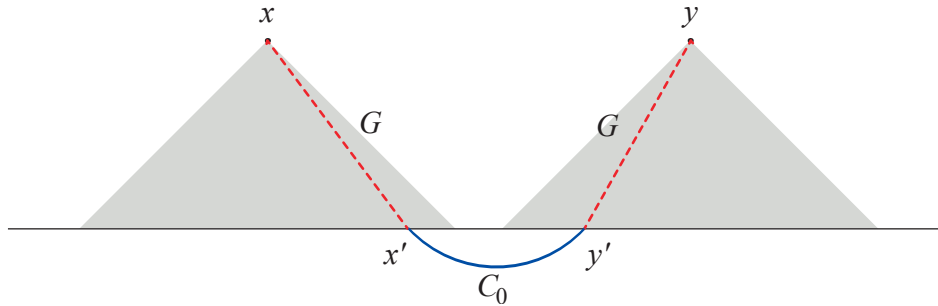


Figure 4. Schematic explanation of the horizon effect

Here we show that the horizon effect is always present in the special case of free relativistic dynamics for any initial state $|\Omega\rangle$ that exhibits exponential clustering of correlations. More precisely the condition is that the dynamics is free in terms of some choice of local fields and the initial state satisfies exponential clustering in terms of the same fields. The horizon effect can be stated mathematically as follows

$$|C_O(x, y; t)| = |\langle \Omega | \mathcal{O}(x, t) \mathcal{O}(y, t) | \Omega \rangle - \langle \Omega | \mathcal{O}(x, t) | \Omega \rangle \langle \Omega | \mathcal{O}(y, t) | \Omega \rangle| < A e^{-(|x-y|-2t)/\xi_h} \quad (14)$$

where the length ξ_h can be called ‘horizon thickness’, A is independent of x and y and as usual we have set the speed of light equal to unit $c = 1$. To demonstrate this relation we focus on the example of Klein-Gordon dynamics, on translationally invariant initial states and choose as local observable the field Φ itself, even though the reasoning holds more generally. Because the Hamiltonian that describes the dynamics is free, the Heisenberg equations of motion are linear which means that they can be solved for general initial conditions using Green’s functions

$$\begin{aligned} \Phi(x, t) &= \int dx' (\partial_t G(x - x', t) \Phi(x') + G(x - x', t) \Pi(x')) \\ &\equiv \sum_{i=0,1} \int dx' G_i(x - x', t) \phi_i(x') \end{aligned} \quad (15)$$

where we denote $\phi_0 = \Phi$, $\phi_1 = \Pi$, $G_0 = \partial_t G$, $G_1 = G$ and the Green’s function is

$$G(x - x', t) = \int \frac{dk}{2\pi} e^{ik(x-x')} \frac{\sin E_k t}{E_k} \quad (16)$$

with $E_k = \sqrt{k^2 + m^2}$. Therefore one obtains

$$C_\Phi(x, y; t) = \sum_{i,j=0,1} \int dx' dy' G_i(x - x', t) G_j(y - y', t) C_{\phi_i, \phi_j}(x', y'; 0) \quad (17)$$

which can be depicted schematically as shown in Fig. 4.

Since the dynamics corresponds to a local relativistically invariant theory, the commutators $[\Phi(x, t), \phi_i(x', 0)]$ vanish outside of the past lightcone i.e. for $|x - x'| > t \geq 0$, which means equivalently that the retarded Green's function $G(x - x', t)$ has support only in the interval $x' \in [x - t, x + t]$. This can be easily verified from (16) by application of Cauchy's theorem and noticing that the integrand is an analytic function of k in the complex k -plane and decays exponentially in the upper or lower half k -plane for $x - x' > t$ or $x - x' < -t$ respectively. Because the initial state satisfies exponential clustering for local field correlations we have

$$|C_{\phi_i, \phi_j}(x', y'; 0)| = |\langle \Omega | \phi_i(x') \phi_j(y') | \Omega \rangle - \langle \Omega | \phi_i(x') | \Omega \rangle \langle \Omega | \phi_j(y') | \Omega \rangle| < c_{ij} e^{-|x' - y'|/\xi_0}$$

where c_{ij} is some constant and ξ_0 is the correlation length characterising the initial state. Substituting in (17) and taking into account the support of the functions G_i we deduce that

$$|C_\Phi(x, y; t)| < A e^{-(|x-y|-2t)/\xi_0}$$

where $A = \sum_{i,j=0,1} c_{ij} \int dx' |G_i(x', t)| \int dy' |G_j(y', t)|$ is independent of x and y .

This proves (14) and shows that for the free case the horizon thickness ξ_h is equal to the initial correlation length ξ_0 .

Further numerical results

The horizon violation effect as presented in Fig. 1 in the main text is characterised by the following features. First of all, it extends through the whole system – correlations do not appear to decay with the distance at all. This is confirmed by the exact analytical calculation based on Bosonisation, as explained in the main text and exposed into detail in the next section of this SI. Second, the out-of-horizon correlations exhibit time oscillations between zero and some maximum value.

In order to clarify further properties of the horizon violation effect, we present in this section additional plots of the dynamics of correlations computed numerically using the TCSA method.

Violation universally present in quenches to the sine-Gordon model

The horizon violation is not restricted to Klein-Gordon to sine-Gordon quenches but universally present for other initial states as demonstrated in Fig. 5. The violation was observed in quenches from the massless free boson (CFT) and in SG to SG quenches both in mass μ and interaction β . The interpretation is that any quench to the SG model or any global change of a parameter introduces entanglement between soliton – anti-soliton pairs resulting in infinite range correlations.

Some details of the effect do change for different initial states, such as the overall sign of the correlations if the quench is from a higher value of the μ or β parameter to a lower one as compared to the opposite direction. This sign flip is quite generic: it is also present in free KG to KG quenches which show no horizon violation. Another interesting detail is the dependence on boundary conditions, discussed below.

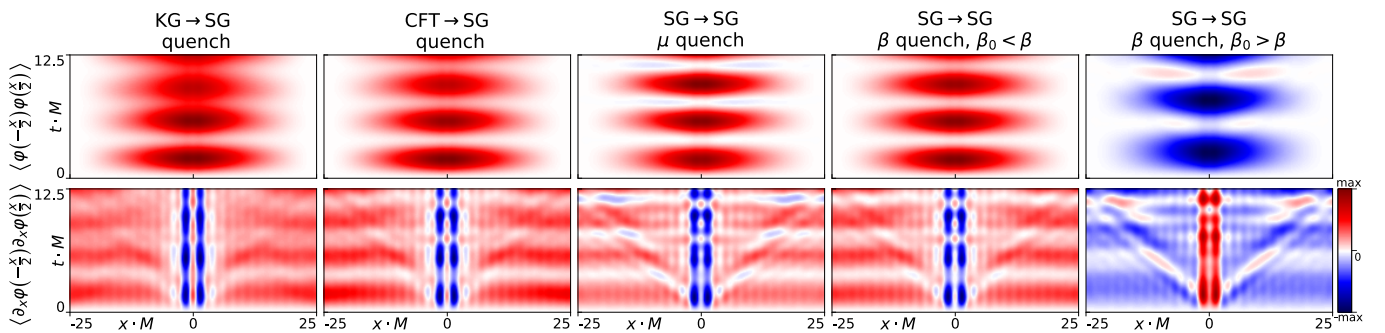


Figure 5. Density plots of correlation dynamics for different types of quenches: from the KG ground state, the massless free boson (CFT) ground state, SG mass μ quench, SG interaction quench from smaller to larger interaction β or vice versa. Plots are for Dirichlet boundary conditions where it is technically easier to perform a TCSA simulation for all these different types of quench.

Sensitivity to boundary conditions

The horizon violation has an interesting sensitivity to boundary conditions as shown in Fig. 6. For Dirichlet boundary conditions the violation is dominated by correlations of the $\partial_x \Phi$ field, while for periodic boundary conditions it switches over to Π . This sensitivity to boundary conditions is another confirmation of the topological origin of the phenomenon.

In Fig. 6, the quenches with Dirichlet boundary conditions (Dirichlet BC = DBC) are started from a massive KG ground state which is the canonical example of a state with exponentially decaying correlations and satisfying clustering. This is also the initial state that we use in the analytical solution based on bosonisation. The pre-quench KG mass m_0 is chosen so that the initial correlation length is 1/10 of the system size, $\xi_0/L = 1/10$. For periodic boundary conditions (periodic BC = PBC), however, it is difficult to implement the KG ground state in the TCSA Hilbert space of the SG model due to the infrared divergent zero mode of the boson field, therefore for PBC we study SG to SG quenches in μ . In SG ground states the correlation length is controlled by the mass m_1 of the lightest particle, i.e. the first breather, which depends on the soliton mass M and the interaction $\Delta = \beta^2/8\pi$ as $m_1 = 2M \sin(\pi\Delta/(2 - 2\Delta))$. The soliton mass itself can be related to the Hamiltonian parameters using Zamolodchikov's mass – coupling relation [36]. We choose the pre-quench μ_0 so that $m_1 L = 10$ and we thus again have $\xi_0/L = 1/10$. Note that due to the zero mode the field Φ is not unambiguously defined for periodic BC and so we only compute correlations of the derivative fields ($\partial_x \Phi$ and $\Pi = \partial_t \Phi$ from the TCSA).

The features of the horizon violation observed for PBC agree with our analytical solution which was also performed for PBC, however starting from a KG ground state, since the ground state of the interacting SG model is not accessible with state of the art analytic techniques. As we have discussed, the features of the effect do not depend qualitatively on the choice of the pre-quench state.

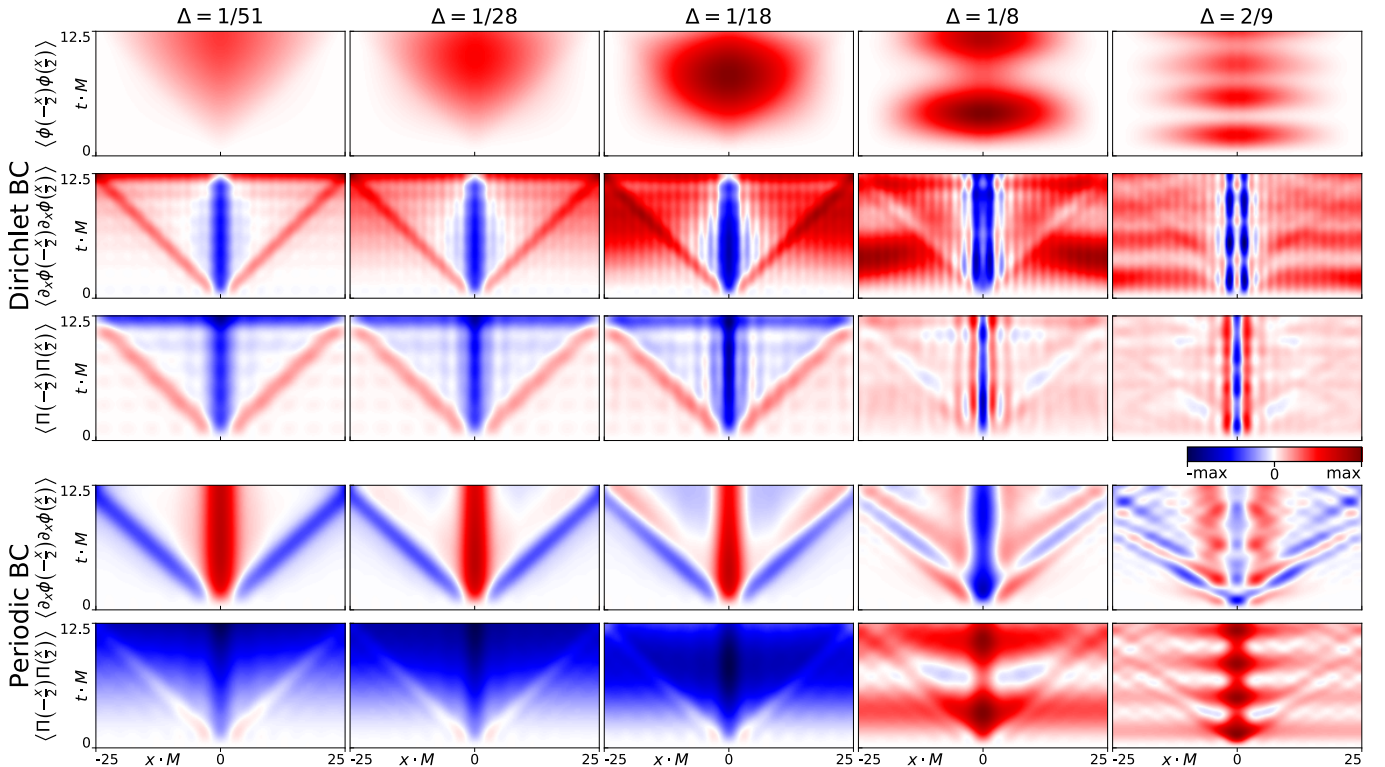


Figure 6. Numerical TCSA simulations demonstrating how the presence of the effect in different observables depends on the boundary conditions imposed on the system.

Properties of horizon violation in the attractive regime

The SG model has a rich variety of physical behaviours: for $\beta^2 < 4\pi$ the interaction between solitons is attractive and they can form bound states (breathers), for $\beta^2 = 4\pi$, the so-called free fermion line, the interaction between solitons vanishes, for $\beta^2 > 4\pi$ it is repulsive and in the vicinity of $\beta^2 \approx 8\pi$ the model undergoes a Berezinskii-Kosterlitz-Thouless type phase transition to a gapless phase where the interaction is irrelevant. Our analytical solution explains the mechanism of the horizon

violation effect at the free fermion line. There, the effect is a consequence of entanglement between soliton – anti-soliton pairs, a four body process. This manifests itself in the frequency of out-of-horizon oscillations of correlations, which was demonstrated with our solution to be $4M$ – four times the soliton mass. This picture is expected to stay valid beyond the free fermion point into the repulsive regime $\beta^2 > 4\pi$. In the attractive regime, however, one can generally expect a different behaviour due to the presence of bound states.

To shed light on this matter, we performed a frequency analysis of the oscillations in the TCSA data for quenches in the attractive regime, as shown in Fig. 7. The data suggest that the oscillation frequency in this case is $2m_1$, i.e. twice the mass of the lightest breather B_1 , which reduces to $4M$ at the free fermion point, consistently with the analytical result. This suggests that in the attractive regime, the violation of horizon is predominantly mediated by entangled pairs of B_1 instead of unbound soliton – anti-soliton pairs. Such an interpretation leads to a prediction: In the free fermion case and in the repulsive regime, the continuous spectrum of the soliton – anti-soliton pairs leads to dephasing and thus to the time-decay of the out-of-horizon component as observed in the analytical calculation. In the attractive regime on the other hand, this dephasing effect is expected to be suppressed due to the fact that breathers are isolated bound state excitations below the two-particle continuum. We therefore expect that there should be no decay of the out-of-horizon component or it should be significantly slower. This expectation seems to be consistent with the TCSA plots, even though our observation of the effect is limited by the finite system size. Detailed study of these characteristics is left for future work.

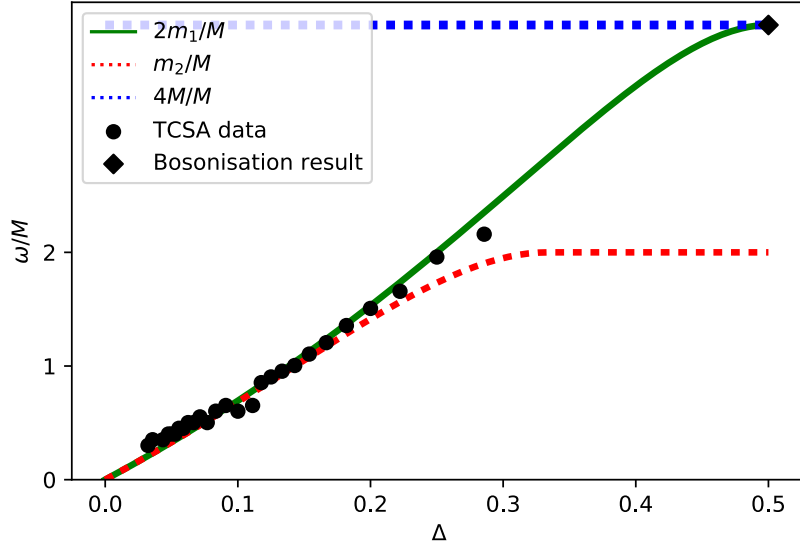


Figure 7. Oscillation frequencies of the horizon violation effect. Numerical data from the TCSA and the analytical result at the free fermion point using bosonisation, are compared with several relevant masses present in the theory: twice the mass of the first breather $2m_1$, mass of the second breather m_2 and four times the soliton mass $4M$. The TCSA works best in the small and intermediate Δ regime and becomes progressively less convergent for $\Delta \gtrsim 0.3$.

Technical details of the TCSA simulations

As explained in the Methods, the TCSA simulations are based on a suitable truncation of the Hilbert space, so that the computation is performed by operations on finite size matrix representations of the Hamiltonians, states and observables. The CFT eigenstate basis is used as basis of the truncated Hilbert space and an energy cutoff is used for the truncation (we refer the reader to [21] for a detailed presentation of the method). The quality of the computed results is confirmed by analysing the convergence of the data for increasing values of the truncation cutoff. For the purposes of the present study we used TCSA bases of dimension 20000 to 28000 states. The rate of convergence was fast enough for all parameter values used in the present work, and we checked that the results have converged sufficiently well for the above values of truncated basis dimensions (cf. also [21]).

The high energy cut-off leads to truncation errors in the computed energy spectra and observables. These errors decrease when the cut-off is increased and the rate of convergence depends on the parameters of the quench: it is better for smaller quenches and for smaller values of the post-quench interaction parameter Δ . Truncation errors generally increase from left to right in the

sequence of density plots of Fig. 1 and 6. They also depend on the choice of observable and are stronger for $\partial_x \Phi$ and Π than for Φ , due to the derivative enhancing the contribution of large wave-number modes. Moreover they are stronger at short distances (i.e. in a narrow central part of the density plots) due to the presence of universal short-distance singularities, however this is not relevant for the horizon effect and its violation which take place at intermediate to large distances. In the present computation the maximum wave-numbers k_{cut} used (which determine the finest spatial resolution L/k_{cut} that can be achieved) range between 28 and 30 in the DBC case and between 11 and 12 in the PBC case, for the same order of truncated space dimension. The truncation errors in the spectrum also lead to the unitary time evolution getting out of phase at larger times, since it is governed by frequencies determined by the energy level differences. However, in this work we are interested in short time scales $t < L/2$, where this effect does not play an important role.

Analytical demonstration of the out-of-horizon effect

In this section we give more details about the analytical solution of the quench from the Klein-Gordon model to the sine-Gordon model that we presented in the main text. Quenches in sine-Gordon have been studied in [37–41] for certain types of initial states. These earlier studies relied on expressing the initial state in the post-quench basis. In contrast, here we use an approach that derives directly the dynamics of correlations from initial ones [42–46] which in the present case relies upon the exact correspondence between the sine-Gordon and massive Thirring models. We follow the three conceptual steps outlined in the Methods section:

1. Fermionising the sine-Gordon model,
2. Computing the dynamics of the correlation functions in terms of initial fermionic correlations,
3. Deriving the initial fermionic correlations from the bosonic ones.

Finally we discuss how to extract exact asymptotic expressions for the connected correlations functions at large distances and clarify in this way the origin of the observed out-of-horizon effect.

Fermionising the sine-Gordon model

Due to strong coupling, the dynamics of the sine-Gordon theory cannot be accessed perturbatively. The model is integrable but the current state of the art methods of the theory of integrability do not allow for computation of dynamical multi-point correlation functions. Our solution therefore relies on a powerful analytical tool, the theory of bosonisation.

Bosonisation is an example of QFT dualities, which allow studying strongly interacting QFTs. The idea is to introduce a nonlinear field transformation, such that the original strongly-interacting model is mapped into a weakly or non-interacting model in terms of the new fields. In modern theoretical physics, dualities play a central role in understanding the physics of quantum fields and unveiling the deeper symmetries of Nature. Bosonisation establishes a mapping between two different (1+1)-dimensional QFTs, one of which is bosonic and the other fermionic. This is achieved through an isomorphism between the Hilbert spaces and the operators of the theories. This isomorphism can be rigorously established for a finite system of size L [23]; however, one can take the thermodynamic limit $L \rightarrow \infty$ in closed form.

The sine-Gordon model is a bosonic theory governed by the Hamiltonian

$$H_{SG} = \int \left(\frac{1}{2} \Pi^2 + \frac{1}{2} (\partial_x \Phi)^2 - \frac{\mu^2}{\beta^2} \cos \beta \Phi \right) dx \quad (18)$$

which can be mapped to a fermionic theory called the massive Thirring model:

$$H_{MT} = \int [\bar{\Psi} (-i\gamma^1 \partial_x + M) \Psi + \frac{1}{2} g (\bar{\Psi} \gamma^\mu \Psi) (\bar{\Psi} \gamma_\mu \Psi)] dx \quad (19)$$

The relation between the couplings is given by [25]:

$$\frac{\beta^2}{4\pi} = \frac{1}{1 + g/\pi},$$

At the so-called "free fermion point" $\beta = \sqrt{4\pi}$ the Thirring interaction vanishes and the dual theory of the SG model is thus the theory of a free Dirac fermion field governed by the Dirac Hamiltonian:

$$H_{MF} = \int \bar{\Psi} (-i\gamma^1 \partial_x + M) \Psi dx, \quad (20)$$

for which the time evolution dynamics can be calculated analytically.

Equivalence of Hilbert spaces

Consider a fermionic field theory described by a set of momentum modes $c_{k,\sigma}$, $k \in \mathbb{Z}$, $\sigma = \pm$, satisfying canonical anti-commutation relations. Further, we assume that the vacuum of the theory is given by the Fermi sea for which all momentum modes with $k \leq 0$ are occupied, while the ones with $k > 0$ are empty. Then any excitation on top of the Fermi sea can be decomposed into a part that merely changes the expectation value of the fermionic number operator and a part containing only particle-hole excitations. The particle-hole excitation operators:

$$a_k^\dagger = \frac{i}{\sqrt{|n_k|}} \sum_{n_q=-\infty}^{\infty} c_{q+|k|,\sigma}^\dagger c_{q,\sigma} \quad \text{with } \sigma = -\text{sign}(k) \quad (21)$$

have all the algebraic properties of bosonic excitation operators. The fermionic Hilbert space can thus be decomposed as:

$$\mathcal{H}_{\text{Fermi}} = \mathcal{H}_{N_-,N_+} \otimes \mathcal{H}_{\text{Bose}} \quad (22)$$

where the states in \mathcal{H}_{N_-,N_+} correspond to sectors with different expectation values of the number operator N_σ and $\mathcal{H}_{\text{Bose}}$ is spanned by all possible particle-hole excitations. The bosonic character of the particle-hole excitations also enables us to construct operator identities between fermionic and bosonic fields.

Bosonisation identities

We can expand the boson field compactified to the radius R as

$$\Phi(x) = \Phi_0 + \frac{RW}{L}x - \frac{1}{\sqrt{L}} \sum_{\substack{n_k=-\infty \\ n_k \neq 0}}^{\infty} \frac{1}{\sqrt{2|k|}} (a_k + a_{-k}^\dagger) e^{ikx} \quad (23)$$

with $k = \frac{2\pi}{L}n_k$ and $[a_k, a_l^\dagger] = \delta_{k,l}$ and W the winding operator. It satisfies $\Phi \sim \Phi + 2\pi R$; in case of the SG model, a convenient choice for the compactification radius is $R = \sqrt{4\pi}/\beta$. The $k \neq 0$ part can be decomposed into two ($\sigma = \pm$) components:

$$\Phi_\sigma(x) = -\frac{1}{\sqrt{4\pi}} \sum_{n_k=1}^{\infty} \frac{1}{\sqrt{n_k}} (a_{-\sigma k} e^{-\sigma ikx} + a_{-\sigma k}^\dagger e^{\sigma ikx}). \quad (24)$$

The $\sigma = \pm$ components can be easily identified as the left/right moving components of the Φ field when it is time evolved under the free massless boson Hamiltonian H_{CFT} :

$$e^{+iH_{CFT}t} \Phi_\sigma(x) e^{-iH_{CFT}t} = \Phi_\sigma(x + \sigma t) \quad (25)$$

The canonical momentum field $\Pi(x)$ is:

$$\Pi(x) = \Pi_0 - \frac{i}{\sqrt{L}} \sum_{\substack{n_k=-\infty \\ n_k \neq 0}}^{\infty} \sqrt{\frac{|k|}{2}} (-a_k + a_{-k}^\dagger) e^{ikx} \quad (26)$$

with Π_0 the zero mode of the canonical momentum field.

The fermion field

$$\Psi = \begin{pmatrix} \Psi_- \\ \Psi_+ \end{pmatrix}$$

satisfying canonical anti-commutation relations and anti-periodic (Neveu-Schwarz) boundary conditions has the following mode expansion:

$$\Psi_\sigma(x) = \frac{1}{\sqrt{L}} e^{\sigma i \frac{\pi}{L} x} \sum_{n_k=-\infty}^{\infty} c_{k,\sigma} e^{-\sigma ikx} \quad (27)$$

with $\sigma = \pm$, $k = \frac{2\pi}{L}n_k$ and $\{c_{k,\sigma}, c_{l,\rho}^\dagger\} = \delta_{\sigma,\rho} \delta_{k,l}$. If evolved with the massless Dirac Hamiltonian $H_{0F} = -i \int \bar{\Psi} \gamma^1 \partial_x \Psi dx$ the $\sigma = \pm$ modes are the left and right-moving components:

$$e^{+iH_{0F}t} \Psi_\sigma(x) e^{-iH_{0F}t} = \Psi_\sigma(x + \sigma t). \quad (28)$$

The fermionic number operator is given by:

$$N_\sigma \equiv \sum_{n_k=-\infty}^{\infty} :c_{k,\sigma}^\dagger c_{k,\sigma}:$$

and acts on the states in \mathcal{H}_{N_-, N_+} as $N_\sigma |n_-, n_+\rangle = n_\sigma |n_-, n_+\rangle$. Bosonisation is defined by an exact operator identity between boson and fermion fields that follows from (21):

$$\Psi_\sigma(x) = \frac{1}{\sqrt{L}} F_\sigma e^{-\sigma i \frac{2\pi}{L} (N_\sigma - \frac{1}{2}) x} : e^{-\sigma i \sqrt{4\pi} \Phi_\sigma(x)} : \quad (29)$$

To ensure that the expression in the r.h.s. of the equation acts in the Hilbert space (22) identically as the fermion field (27), it is composed of a bosonic part ($: e^{-\sigma i \sqrt{4\pi} \Phi_\sigma(x)} :$) that acts upon $\mathcal{H}_{\text{Bose}}$ and a part ($F_\sigma e^{-i \frac{2\pi}{L} (N_\sigma - \frac{1}{2}) x}$) that acts upon \mathcal{H}_{N_-, N_+} . The exponentials of the bosonic fields are known as vertex operators, while the operators F_σ are the Klein factors which act as hopping operators between different N_σ sectors:

$$F_\sigma^\dagger |n_-, n_+\rangle \otimes |\psi\rangle_{\text{Bose}} \equiv (-1)^{n_- + \delta_{\sigma,+} n_+} |n_- + \delta_{\sigma,-}, n_+ + \delta_{\sigma,+}\rangle \otimes |\psi\rangle_{\text{Bose}}$$

and have the following algebraic properties:

$$\begin{aligned} [F_\sigma, a_k^\dagger] &= [F_\sigma, a_k] = 0 \\ \{F_\sigma^\dagger, F_\rho\} &= 2\delta_{\sigma,\rho}, \quad \forall \sigma, \rho \quad (\text{with } F_\rho F_\rho^\dagger = F_\rho^\dagger F_\rho = 1) \\ \{F_\sigma^\dagger, F_\rho^\dagger\} &= \{F_\sigma, F_\rho\} = 0, \quad \sigma \neq \rho \\ [N_\sigma, F_\rho^\dagger] &= \delta_{\sigma,\rho} F_\rho^\dagger, \quad [N_\sigma, F_\rho] = -\delta_{\sigma,\rho} F_\rho \end{aligned} \quad (30)$$

where the semicolon denotes the usual normal ordering of the bosonic modes. In terms of the fermions, the bosonic zero modes are given as

$$RW = \sqrt{\pi}(N_- + N_+), \quad \Pi_0 = \frac{\sqrt{\pi}}{L}(-N_- + N_+). \quad (31)$$

$$(32)$$

Formally, the bosonisation identity is proven for systems of finite size L . We therefore derive all the expressions in finite volume and take the thermodynamic limit $L \rightarrow \infty$ in the end. The inverse relations of (29) expressing the bosonic fields in terms of the fermionic ones are given by:

$$\begin{aligned} \partial_x \Phi(x) &= \sqrt{\pi} \sum_{\sigma=\pm} : \Psi_\sigma^\dagger(x) \Psi_\sigma(x) :, \\ \Pi(x) &= \sqrt{\pi} \sum_{\sigma=\pm} \sigma : \Psi_\sigma^\dagger(x) \Psi_\sigma(x) :. \end{aligned} \quad (33)$$

Sine-Gordon correlations at the free fermion point

Using the above relations we can fermionise the sine-Gordon model (18) at $\beta = \sqrt{4\pi}$ to obtain the free massive Dirac Hamiltonian (20). Exploiting (33), the connected correlation functions of the fields $\partial_x \Phi$ and Π can be expressed as:

$$\begin{aligned} \langle \Omega | \partial_x \Phi(x, t) \partial_y \Phi(y, t) | \Omega \rangle_c &= \pi \sum_{\sigma, \rho=\pm} \left(\langle \Omega | : \Psi_\sigma^\dagger(x, t) \Psi_\sigma(x, t) : : \Psi_\rho^\dagger(y, t) \Psi_\rho(y, t) : | \Omega \rangle - \right. \\ &\quad \left. - \langle \Omega | : \Psi_\sigma^\dagger(x, t) \Psi_\sigma(x, t) : | \Omega \rangle \langle \Omega | : \Psi_\rho^\dagger(y, t) \Psi_\rho(y, t) : | \Omega \rangle \right), \end{aligned} \quad (34)$$

and:

$$\begin{aligned} \langle \Omega | \Pi(x, t) \Pi(y, t) | \Omega \rangle_c &= \pi \sum_{\sigma, \rho=\pm} \sigma \rho \left(\langle \Omega | : \Psi_\sigma^\dagger(x, t) \Psi_\sigma(x, t) : : \Psi_\rho^\dagger(y, t) \Psi_\rho(y, t) : | \Omega \rangle - \right. \\ &\quad \left. - \langle \Omega | : \Psi_\sigma^\dagger(x, t) \Psi_\sigma(x, t) : | \Omega \rangle \langle \Omega | : \Psi_\rho^\dagger(y, t) \Psi_\rho(y, t) : | \Omega \rangle \right), \end{aligned} \quad (35)$$

We also use the identity

$$\langle \Omega | : A : : B : | \Omega \rangle - \langle \Omega | : A : | \Omega \rangle \langle \Omega | : B : | \Omega \rangle = \langle \Omega | A B | \Omega \rangle - \langle \Omega | A | \Omega \rangle \langle \Omega | B | \Omega \rangle \quad (36)$$

to eliminate the normal ordering of $: \Psi^\dagger \Psi :$ pairs in fermionised expressions for correlation functions. This equality follows from $: A := A - \langle 0 | A | 0 \rangle$ where $|0\rangle$ is the vacuum state.

Computing the dynamics of correlation functions

Free fermion dynamics

As anticipated, using the bosonisation identities (29) and (33), the sine-Gordon Hamiltonian at $\beta = \sqrt{4\pi}$ is mapped to the Dirac Hamiltonian (20), more precisely in the form:

$$H_{MF} = \sum_{\sigma} \int dx (\sigma i : \Psi_{\sigma}^{\dagger} \partial_x \Psi_{\sigma} : - M : \Psi_{\sigma}^{\dagger} \Psi_{-\sigma} :)$$

The equations of motion are:

$$\dot{\Psi}_{\sigma} = \sigma \partial_x \Psi_{\sigma} + iM \Psi_{-\sigma}$$

which can be solved exactly for arbitrary initial conditions. The solution in infinite volume can be expressed in the form where the initial fields are propagated with the retarded Green's functions

$$\Psi_{\sigma}(x, t) = \sum_{\sigma'=\pm} \int_{-\infty}^{\infty} dx' G_{\sigma\sigma'}(x-x', t) \Psi_{\sigma'}(x') \quad (37)$$

where

$$G_{\sigma,\sigma'}(x-x', t) = \Theta(t) \int \frac{dk}{2\pi} e^{ik(x-x')} \left[\delta_{\sigma,\sigma'} \cos(E_k t) + (\sigma i k \delta_{\sigma,\sigma'} + iM \delta_{\sigma,-\sigma'}) \frac{\sin(E_k t)}{E_k} \right] \quad (38)$$

with $E_k = \sqrt{k^2 + M^2}$.

Note that the Green's function is Lorentz invariant and it vanishes out of the light-cone, i.e. for $|x-x'| > t$. For $t=0$ it is $G_{\sigma\sigma'}(x-x', 0) = \delta_{\sigma,\sigma'} \delta(x-x')$ and in the special case $M=0$ it reduces to $\delta_{\sigma,\sigma'} \delta(x+\sigma t-x')$ as it should.

The propagator can be evaluated explicitly [47]:

$$\begin{aligned} G_{\sigma\sigma'}(x, t) &= \frac{1}{2} \Theta(t) \left(\delta_{\sigma,\sigma'} (\partial_t + \sigma \partial_x) + iM \delta_{\sigma,-\sigma'} \right) \left(\Theta(t^2 - x^2) J_0(M \sqrt{t^2 - x^2}) \right) \\ &= \Theta(t) \left\{ \frac{1}{2} M \Theta(t^2 - x^2) \left[\delta_{\sigma,\sigma'} (-t + \sigma x) \frac{J_1(M \sqrt{t^2 - x^2})}{\sqrt{t^2 - x^2}} + i \delta_{\sigma,-\sigma'} J_0(M \sqrt{t^2 - x^2}) \right] + \delta_{\sigma,\sigma'} \delta(x + \sigma t) \right\} \quad (39) \end{aligned}$$

where J_0 and J_1 are the Bessel functions of zeroth and first order respectively.

Dynamics of correlation functions

Substituting (37) into (34) and (35) and using (36) yields

$$\begin{aligned} \langle \Omega | \partial_x \Phi(x, t) \partial_y \Phi(y, t) | \Omega \rangle_c &= \\ \pi \sum_{\sigma, \rho, \sigma_i, \rho_i = \pm} \int dx_1 dx_2 dy_1 dy_2 G_{\sigma\sigma_1}^*(x-x_1, t) G_{\sigma\sigma_2}(x-x_2, t) G_{\rho\rho_1}^*(y-y_1, t) G_{\rho\rho_2}(y-y_2, t) \times \\ &\times \left(\langle \Omega | \Psi_{\sigma_1}^{\dagger}(x_1) \Psi_{\sigma_2}(x_2) \Psi_{\rho_1}^{\dagger}(y_1) \Psi_{\rho_2}(y_2) | \Omega \rangle - \langle \Omega | \Psi_{\sigma_1}^{\dagger}(x_1) \Psi_{\sigma_2}(x_2) | \Omega \rangle \langle \Omega | \Psi_{\rho_1}^{\dagger}(y_1) \Psi_{\rho_2}(y_2) | \Omega \rangle \right). \end{aligned} \quad (40)$$

and

$$\begin{aligned} \langle \Omega | \Pi(x, t) \Pi(y, t) | \Omega \rangle_c &= \\ \pi \sum_{\sigma, \rho, \sigma_i, \rho_i = \pm} \sigma \rho \int dx_1 dx_2 dy_1 dy_2 G_{\sigma\sigma_1}^*(x-x_1, t) G_{\sigma\sigma_2}(x-x_2, t) G_{\rho\rho_1}^*(y-y_1, t) G_{\rho\rho_2}(y-y_2, t) \times \\ &\times \left(\langle \Omega | \Psi_{\sigma_1}^{\dagger}(x_1) \Psi_{\sigma_2}(x_2) \Psi_{\rho_1}^{\dagger}(y_1) \Psi_{\rho_2}(y_2) | \Omega \rangle - \langle \Omega | \Psi_{\sigma_1}^{\dagger}(x_1) \Psi_{\sigma_2}(x_2) | \Omega \rangle \langle \Omega | \Psi_{\rho_1}^{\dagger}(y_1) \Psi_{\rho_2}(y_2) | \Omega \rangle \right). \end{aligned} \quad (41)$$

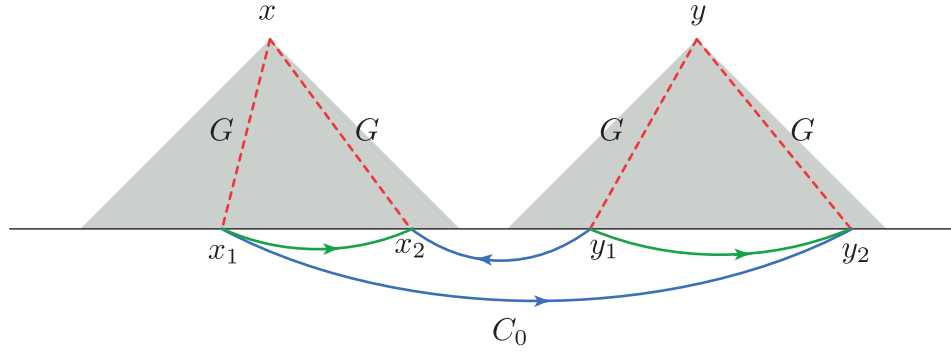


Figure 8. Diagrammatic representation of the convolution formulas (40) and (41) for the derivation of dynamics of correlations at the free fermion point. The dashed red lines denote the propagators, the blue and green lines denote the Klein factor contractions corresponding to the initial fermionic correlations.

Initial fermionic correlation functions

The last step is to construct the initial fermionic correlation functions

$$\begin{aligned} C_{\sigma_1\sigma_2\rho_1\rho_2}(x_1, x_2, y_1, y_2) &\equiv \langle \Omega | \Psi_{\sigma_1}^\dagger(x_1) \Psi_{\sigma_2}(x_2) \Psi_{\rho_1}^\dagger(y_1) \Psi_{\rho_2}(y_2) | \Omega \rangle \\ C_{\sigma_1\sigma_2}(x_1, x_2) &\equiv \langle \Omega | \Psi_{\sigma_1}^\dagger(x_1) \Psi_{\sigma_2}(x_2) | \Omega \rangle. \end{aligned} \quad (42)$$

entering (40) and (41).

Initial state

The state $|\Omega\rangle$ that we are quenching from is the ground state of the Klein-Gordon model

$$H_{KG} = \int \left(\frac{1}{2} \Pi^2 + \frac{1}{2} (\partial_x \Phi)^2 + \frac{1}{2} m_0^2 \Phi^2 \right) dx.$$

When embedded in the fermionic Hilbert space (22) the state $|\Omega\rangle$ only has excitations of bosonic particle-hole type:

$$|\Omega\rangle_{\mathcal{H}_{\text{Fermi}}} = |0, 0\rangle \otimes |\Omega\rangle.$$

In (34), (35) and all other fermionic expressions we drop the index $\mathcal{H}_{\text{Fermi}}$ for simplicity of notation but always have $|\Omega\rangle_{\mathcal{H}_{\text{Fermi}}}$ in mind when we write $|\Omega\rangle$.

Fermionic superselection rules

Using the bosonisation identity (29), the initial fermionic correlations (42) can be expressed in terms of bosonic fields. Collecting together all Klein factors entering in $C_{\sigma_1\sigma_2\rho_1\rho_2}(x_1, x_2, y_1, y_2)$ and $C_{\sigma_1\sigma_2}(x_1, x_2)$ using the algebraic relations (30) and commuting the Klein factors past the $e^{-i\frac{2\pi}{L}(N_\sigma - \frac{1}{2})x}$ factors from (29) using the identity $e^{AB} = B e^{A+c}$ if $[A, B] = cB$ for $c \in \mathbb{C}$ gives the following phases:

$$\Theta_{\sigma_1\sigma_2\rho_1\rho_2}(x_1, x_2, y_1, y_2) \equiv e^{i\frac{2\pi}{L} [\sigma_1(\frac{1}{2} - \delta_{\sigma_1, \sigma_2} + \delta_{\sigma_1, \rho_1} - \delta_{\sigma_1, \rho_2})x_1 - \sigma_2(-\frac{1}{2} + \delta_{\sigma_2, \rho_1} - \delta_{\sigma_2, \rho_2})x_2 + \rho_1(\frac{1}{2} - \delta_{\rho_1, \rho_2})y_1 + \frac{1}{2}\rho_2 y_2]} \quad (43)$$

for $C_{\sigma_1\sigma_2\rho_1\rho_2}$ and and

$$\Theta_{\sigma_1\sigma_2}(x_1, x_2) = e^{i\frac{2\pi}{L} [\sigma_1(\frac{1}{2} - \delta_{\sigma_1, \sigma_2})x_1 + \frac{1}{2}\sigma_2 x_2]} \quad (44)$$

for $C_{\sigma_1\sigma_2}$. Both of these phases become identically equal to 1 once we take the thermodynamic limit $L \rightarrow \infty$.

The Klein factors impose the following superselection rules when contracted with the $\mathcal{H}_{\hat{N}}$ part of $|\Omega\rangle$:

$$\langle 0, 0 | F_{\sigma_1}^\dagger F_{\sigma_2} F_{\rho_1}^\dagger F_{\rho_2} | 0, 0 \rangle = \delta_{\sigma_1, \sigma_2} \delta_{\rho_1, \rho_2} + \delta_{\sigma_1, \rho_2} \delta_{\sigma_2, \rho_1} (1 - \delta_{\sigma_1 \sigma_2}). \quad (45)$$

This means that any fermion F_σ appearing in the expression must be matched with an antifermion F_σ^\dagger of the same type σ , or in other words the string of operators must preserve the total $N_+ = 0$ and $N_- = 0$. Therefore the only non-vanishing combinations are C_{++++} , C_{+---} , C_{+--+} and those with all signs reversed. For the two-point functions we have:

$$\langle 0, 0 | F_{\sigma_1}^\dagger F_{\sigma_2} | 0, 0 \rangle = \delta_{\sigma_1, \sigma_2} \quad (46)$$

so the only nonvanishing combinations are C_{++} and C_{--} .

Contracting vertex operators

We therefore end up with the following expressions:

$$\begin{aligned}
C_{\sigma_1\sigma_2\rho_1\rho_2}(x_1, x_2, y_1, y_2) &= \frac{1}{L^2} \left\{ \delta_{\sigma_1, \sigma_2} \delta_{\rho_1, \rho_2} + \delta_{\sigma_1, \rho_2} \delta_{\sigma_2, \rho_1} (1 - \delta_{\sigma_1\sigma_2}) \right\} \Theta_{\sigma_1\sigma_2\rho_1\rho_2}(x_1, x_2, y_1, y_2) \times \\
&\quad \times \left\langle \Omega \left| :e^{+\sigma_1\sqrt{4\pi i}\Phi_{\sigma_1}(x_1)}::e^{-\sigma_2\sqrt{4\pi i}\Phi_{\sigma_2}(x_2)}::e^{+\rho_1\sqrt{4\pi i}\Phi_{\rho_1}(y_1)}::e^{-\rho_2\sqrt{4\pi i}\Phi_{\rho_2}(y_2)}: \right| \Omega \right\rangle \\
C_{\sigma_1\sigma_2}(x_1, x_2) &= \frac{1}{L} \delta_{\sigma_1, \sigma_2} \Theta_{\sigma_1\sigma_2}(x_1, x_2) \left\langle \Omega \left| :e^{+\sigma_1\sqrt{4\pi i}\Phi_{\sigma_1}(x_1)}::e^{-\sigma_2\sqrt{4\pi i}\Phi_{\sigma_2}(x_2)}: \right| \Omega \right\rangle
\end{aligned} \tag{47}$$

In order to evaluate these correlation functions we exploit the fact that, since the initial state $|\Omega\rangle$ is the ground state of Klein Gordon model, it is Gaussian in terms of the bosonic field. For such Gaussian states Wick's theorem yields

$$\left\langle \prod_i e^{ia_i\Phi_{\sigma_i}(x_i)} \right\rangle = e^{-\frac{1}{2} \sum_i a_i^2 \langle \Phi_{\sigma_i}^2(x_i) \rangle - \sum_{i < j} a_i a_j \langle \Phi_{\sigma_i}(x_i) \Phi_{\sigma_j}(x_j) \rangle} \tag{48}$$

Using the Baker-Campbell-Hausdorff formula we obtain an analogous formula for normal-ordered exponentials

$$\left\langle \prod_i :e^{ia_i\Phi_{\sigma_i}(x_i)}: \right\rangle = e^{-\frac{1}{2} \sum_i a_i^2 \langle : \Phi_{\sigma_i}^2(x_i) : \rangle - \sum_{i < j} a_i a_j \langle \Phi_{\sigma_i}(x_i) \Phi_{\sigma_j}(x_j) \rangle} \tag{49}$$

Applying it to our problem results in

$$\begin{aligned}
&\left\langle \Omega \left| :e^{+\sigma_1\sqrt{4\pi i}\Phi_{\sigma_1}(x_1)}::e^{-\sigma_2\sqrt{4\pi i}\Phi_{\sigma_2}(x_2)}::e^{+\sigma_3\sqrt{4\pi i}\Phi_{\rho_1}(x_3)}::e^{-\rho_2\sqrt{4\pi i}\Phi_{\sigma_4}(x_4)}: \right| \Omega \right\rangle = \\
&= \exp \left[-2\pi \sum_{i=1}^4 \langle : \Phi_{\sigma_i}^2 : \rangle_{\Omega} - 4\pi \left(-\sigma_1\sigma_2 \langle \Phi_{\sigma_1}(x_1) \Phi_{\sigma_2}(x_2) \rangle_{\Omega} - \sigma_1\sigma_4 \langle \Phi_{\sigma_1}(x_1) \Phi_{\sigma_4}(x_4) \rangle_{\Omega} - \sigma_2\sigma_3 \langle \Phi_{\sigma_2}(x_2) \Phi_{\sigma_3}(x_3) \rangle_{\Omega} \right. \right. \\
&\quad \left. \left. - \sigma_3\sigma_4 \langle \Phi_{\sigma_3}(x_3) \Phi_{\sigma_4}(x_4) \rangle_{\Omega} + \sigma_1\sigma_3 \langle \Phi_{\sigma_1}(x_1) \Phi_{\sigma_3}(x_3) \rangle_{\Omega} + \sigma_2\sigma_4 \langle \Phi_{\sigma_2}(x_2) \Phi_{\sigma_4}(x_4) \rangle_{\Omega} \right) \right] \\
&\left\langle \Omega \left| :e^{+\sigma_1\sqrt{4\pi i}\Phi_{\sigma_1}(x_1)}::e^{-\sigma_2\sqrt{4\pi i}\Phi_{\sigma_2}(x_2)}: \right| \Omega \right\rangle = \exp \left[-2\pi \sum_{i=1}^2 \langle : \Phi_{\sigma_i}^2 : \rangle_{\Omega} + 4\pi\sigma_1\sigma_2 \langle \Phi_{\sigma_1}(x_1) \Phi_{\sigma_2}(x_2) \rangle_{\Omega} \right]
\end{aligned} \tag{50}$$

where we abbreviated $\langle \Omega | \bullet | \Omega \rangle$ by $\langle \bullet \rangle_{\Omega}$.

Initial two-point functions of bosonic fields

The problem now reduces to calculating the initial two-point correlation functions $\langle \Omega | \Phi_{\sigma_1}(x_1) \Phi_{\sigma_2}(x_2) | \Omega \rangle$, which are correlations between the chiral components of the bosonic field evaluated in the Klein-Gordon ground state. From (24) we find

$$\begin{aligned}
&\langle \Omega | \Phi_{\sigma_1}(x_1) \Phi_{\sigma_2}(x_2) | \Omega \rangle \\
&= \frac{1}{L} \sum_{n_k=1}^{\infty} \left\{ \delta_{\sigma_1, \sigma_2} \left[\frac{1}{2k} e^{-\sigma_1 i k (x_1 - x_2)} + \frac{1}{4k} \left(\frac{E_{0k}}{k} + \frac{k}{E_{0k}} - 2 \right) \cos k(x_1 - x_2) \right] \right. \\
&\quad \left. - \delta_{\sigma_1, -\sigma_2} \frac{1}{4k} \left(\frac{E_{0k}}{k} - \frac{k}{E_{0k}} \right) \cos k(x_1 - x_2) \right\}
\end{aligned} \tag{51}$$

where $E_{0k} = \sqrt{k^2 + m_0^2}$ and the sum runs over discrete momenta, $k = 2\pi n_k/L$, for positive integers n_k . It is easy to verify that for $m_0 = 0$ the only term that does not vanish is the first one: this equals $-\frac{1}{4\pi} \log(1 - e^{-\sigma i 2\pi x/L})$ and is the one that results in the standard CFT ground state correlations.

Putting the building blocks together

Substituting (51) in (50) and then back to (47) we finally find explicit formulae for the non-vanishing initial four-point fermionic correlations

$$\begin{aligned}
C_{\sigma\sigma\sigma\sigma}(x_1, x_2, y_1, y_2) &= \Theta_{\sigma\sigma\sigma\sigma}(x_1, x_2, y_1, y_2) C_{\sigma\sigma\sigma\sigma}^0(x_1, x_2, y_1, y_2) \times \\
&\quad \times \exp \left[4\pi \left(I_1(x_1 - x_2) + I_1(y_1 - y_2) + I_1(x_1 - y_2) + I_1(x_2 - y_1) - I_1(x_1 - y_1) - I_1(x_2 - y_2) \right) \right] \\
C_{\sigma\sigma(-\sigma)(-\sigma)}(x_1, x_2, y_1, y_2) &= \Theta_{\sigma\sigma(-\sigma)(-\sigma)}(x_1, x_2, y_1, y_2) C_{\sigma\sigma(-\sigma)(-\sigma)}^0(x_1, x_2, y_1, y_2) \times \\
&\quad \times \exp \left[4\pi \left(I_1(x_1 - x_2) + I_1(y_1 - y_2) + I_2(x_1 - y_2) + I_2(x_2 - y_1) - I_2(x_1 - y_1) - I_2(x_2 - y_2) \right) \right] \\
C_{\sigma(-\sigma)(-\sigma)\sigma}(x_1, x_2, y_1, y_2) &= \Theta_{\sigma(-\sigma)(-\sigma)\sigma}(x_1, x_2, y_1, y_2) C_{\sigma(-\sigma)(-\sigma)\sigma}^0(x_1, x_2, y_1, y_2) \times \\
&\quad \times \exp \left[4\pi \left(I_2(x_1 - x_2) + I_2(y_1 - y_2) + I_1(x_1 - y_2) + I_1(x_2 - y_1) - I_2(x_1 - y_1) - I_2(x_2 - y_2) \right) \right]
\end{aligned} \tag{52}$$

where $C_{\sigma_1\sigma_2\rho_1\rho_2}^0(x_1, x_2, y_1, y_2)$ denotes the CFT part of the corresponding correlations:

$$\begin{aligned}
C_{\sigma\sigma\sigma\sigma}^0(x_1, x_2, y_1, y_2) &= \frac{1}{L^2} \exp \left[4\pi \left(I_0^\sigma(x_1 - x_2) + I_0^\sigma(y_1 - y_2) + I_0^\sigma(x_1 - y_2) + I_0^\sigma(x_2 - y_1) - I_0^\sigma(x_1 - y_1) - I_0^\sigma(x_2 - y_2) \right) \right] \\
C_{\sigma\sigma(-\sigma)(-\sigma)}^0(x_1, x_2, y_1, y_2) &= \frac{1}{L^2} \exp \left[4\pi \left(I_0^\sigma(x_1 - x_2) + I_0^{-\sigma}(y_1 - y_2) \right) \right] \\
C_{\sigma(-\sigma)(-\sigma)\sigma}^0(x_1, x_2, y_1, y_2) &= \frac{1}{L^2} \exp \left[4\pi \left(I_0^\sigma(x_1 - y_2) + I_0^{-\sigma}(x_2 - y_1) \right) \right].
\end{aligned} \tag{53}$$

The non-vanishing two-point correlations are

$$C_{\sigma\sigma}(x_1, x_2) = \Theta_{\sigma\sigma}(x_1, x_2) C_{\sigma\sigma}^0(x_1, x_2) \exp \left[4\pi I_1(x_1 - x_2) \right], \tag{54}$$

with

$$C_{\sigma\sigma}^0(x_1, x_2) = \frac{1}{L} \exp \left[4\pi I_0^\sigma(x_1 - x_2) \right].$$

The functions I_0^\pm , I_1 and I_2 are given by

$$\begin{aligned}
I_1(x) &:= \frac{1}{L} \sum_{n_k=1}^{\infty} \frac{1}{4k} \left(\frac{E_{0k}}{k} + \frac{k}{E_{0k}} - 2 \right) (\cos kx - 1) \\
I_2(x) &:= \frac{1}{L} \sum_{n_k=1}^{\infty} \frac{1}{4k} \left(\frac{E_{0k}}{k} - \frac{k}{E_{0k}} \right) (\cos kx - 1) \\
I_0^\sigma(x) &:= \frac{1}{L} \sum_{n_k=1}^{\infty} \frac{1}{2k} e^{-\sigma i k x}
\end{aligned} \tag{55}$$

It can be verified that the above formulae reproduce the known fermionic correlations for the massless free fermion (CFT) ground state. In particular, the fermionic antisymmetry property is granted by the canonical anticommutation relations of the fermion field as defined by (29). The $I_0^\sigma(x)$, when evaluated, gives terms $\propto \log L$ that cancel the $\frac{1}{L}$ factors in front of the initial correlations.

The thermodynamic limit $L \rightarrow \infty$ is obtained by replacing the sums in the functions (55) by integrals:

$$\frac{1}{L} \sum_{n_k=1}^{\infty} \rightarrow \int_0^\infty \frac{dk}{2\pi} \tag{56}$$

except when there is an infrared singularity, while the phases $\Theta_{\sigma_1\sigma_2\rho_1\rho_2}$ and $\Theta_{\sigma_1\sigma_2}$ become identically equal to one.

The integrals corresponding to $I_1(x)$ and $I_2(x)$ are infrared and ultraviolet convergent and can easily be evaluated numerically. The expression $I_0^\sigma(x)$ has an infrared divergence and should be kept as a discrete until the end of the calculation. This part is the only one that does not vanish in the case $m_0 = m$ and it is responsible for the CFT ground state correlations. Specifically it can be shown that upon exponentiation

$$\lim_{L \rightarrow \infty} \frac{1}{L} \exp(4\pi I_0^\sigma(x)) = -\frac{\sigma i}{2\pi} \frac{1}{x}, \tag{57}$$

which gives the standard algebraically decaying CFT correlations

$$C_{\sigma\sigma}^0(x_1, x_2) = -\frac{\sigma i}{2\pi} \frac{1}{x_1 - x_2} \quad (58)$$

It is worth noticing that, while both $I_1(x)$ and $I_2(x)$ vanish for $|x| \rightarrow 0$ and therefore do not alter the short distance behaviour of any correlator (which should indeed be controlled by the CFT scaling laws), at large distances their asymptotic behaviour is

$$\begin{aligned} I_1(x) &\sim -\frac{m_0|x|}{16} + \frac{1}{4\pi} \log|x| + c_1 \\ I_2(x) &\sim -\frac{m_0|x|}{16} + c_2 \end{aligned} \quad (59)$$

where c_1, c_2 are numerical constants. These asymptotics precisely cancel the algebraic decay of CFT correlations and switch it to an exponential one, as expected for a massive KG ground state $|\Omega\rangle$.

The initial fermionic correlations can be computed by combining (52), (54) and (55). Substituting in (40) and (41) and using (38) gives the time evolution of the two-point connected correlation function $C_{\partial\Phi}(x, y; t)$. The result of a numerical integration is shown in Fig. 2 of the main text and in Fig. 9, where the correlations of both observables are displayed together for comparison. Note that while the numerical computation is efficient outside of the horizon (for $|x - y| > 2t$), this is not the case inside the horizon (for $|x - y| < 2t$) due to the presence of singularities at $x_1 = y_2$ and $x_2 = y_1$. In this region it is necessary to split the integrands into their singular and non-singular parts and evaluate them separately, noticing that the singular part can be expressed as a sum of products of double integrals (instead of quadruple), which speeds up its evaluation. Moreover a short-distance cutoff $\epsilon \approx 0.1/m_0$ has been used to smear the singularities and make the numerical integration feasible.

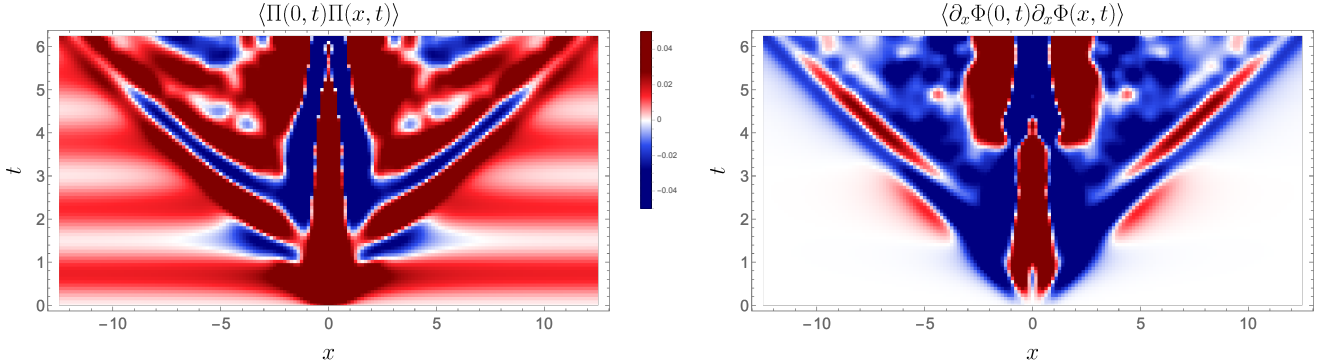


Figure 9. Analytical results from bosonisation for the correlation functions $\langle \Pi(0, t)\Pi(x, t) \rangle$ (left) and $\langle \partial_x \Phi(0, t)\partial_x \Phi(x, t) \rangle$ (right) with SG dynamics at the free fermion point $\beta = \sqrt{4\pi}$ ($\Delta = 1/2$), starting from the Klein-Gordon ground state $|\Omega\rangle$. Notice that the horizon violation effect is present in the correlations of Π , while it is not present for Φ . The initial state is the KG ground state with mass m_0 (used as length and time unit) and the soliton mass $M = 2.5m_0$, as in Fig. 2.

Explanation of the out-of-horizon effect

The asymptotics of connected correlations at any time t and large distance $r = |x - y|$ can be derived using (52), (54), (55), (40), (41) and (38). From (40), (41) and the fact that the fermionic propagators have support only inside the lightcones it follows that the large distance asymptotics outside of the horizon lines $r = 2t$ are determined by the asymptotics of the initial four-point fermionic correlations as the distance between the pairs of coordinates x_1, x_2 and y_1, y_2 becomes large. The asymptotic expansions (59) imply that the cross-terms $C_{\sigma(-\sigma)(-\sigma)\sigma}$ do not tend to $C_{\sigma(-\sigma)}C_{(-\sigma)\sigma}$ (which vanishes due to the Klein factor superselection rules), but they have a non-zero limit instead

$$\lim_{r \rightarrow \pm\infty} C_{\sigma(-\sigma)(-\sigma)\sigma}(x_1, x_2, y_1 + r, y_2 + r) = \frac{A}{(2\pi)^2} e^{4\pi I_2(x_1 - x_2) + 4\pi I_2(y_1 - y_2)} \neq C_{\sigma(-\sigma)}(x_1, x_2)C_{(-\sigma)\sigma}(y_1, y_2) = 0 \quad (60)$$

where $A = \exp[8\pi(c_1 - c_2)]$ and c_1, c_2 are the constants defined in (59). This is in contrast with the behaviour of $C_{\sigma\sigma\sigma\sigma}$ and $C_{\sigma\sigma(-\sigma)(-\sigma)}$ correlations, which factorise at large distances to $C_{\sigma\sigma}C_{\sigma\sigma}$ and $C_{\sigma\sigma}C_{(-\sigma)(-\sigma)}$ respectively.

The above violation of clustering implies the dynamical emergence of infinite range correlations presented in the main text. More specifically, from (40), (41) and (60) the asymptotic values of the connected correlation functions $C_{\partial\Phi}(x, y; t)$

and $C_{\Pi}(x, y; t)$ at large distance $r = |x - y|$ are

$$\lim_{r \rightarrow \infty} C_{\partial\Phi}(0, r; t) = 0 \quad (61)$$

$$\lim_{r \rightarrow \infty} C_{\Pi}(0, r; t) = \frac{A}{2\pi} \left| \sum_{\sigma} \sigma \int dx_1 dx_2 G_{\sigma,+1}^*(x_1, t) G_{\sigma,-1}(x_2, t) e^{4\pi I_2(x_1 - x_2)} \right|^2 \quad (62)$$

At $t = 0$ the Green's functions (38) corresponding to the time evolution of the cross-terms vanish, so these terms do not contribute to the initial state. For $t > 0$ they are propagated by the off-diagonal part of the Green's functions. As we can easily see by the stationary phase method, the above expression is oscillatory and decays with time as

$$\lim_{r \rightarrow \infty} C_{\Pi}(0, r; t) \sim \frac{AB^2M}{(4\pi)^2} \frac{(1 + \sin 4Mt)}{t} \quad \text{for } t \rightarrow \infty \quad (63)$$

with $B = \int_{-\infty}^{+\infty} e^{4\pi I_2(s)} ds$. We remark that the leading correction to this asymptotic value at large distances turns out to decay exponentially with the distance.